

Diversity and activity of nitrogen-fixing communities across ocean basins

Mary R. Gradoville ^{1,*}, Deniz Bombar,^{2,b} Byron C. Crump,¹ Ricardo M. Letelier,¹ Jonathan P. Zehr,² Angelicque E. White¹

¹College of Earth, Ocean, and Atmospheric Sciences, Oregon State University, Corvallis, Oregon

²Ocean Sciences Department, University of California Santa Cruz, Santa Cruz, California

Abstract

Recent observations of N₂ fixation rates (NFR) and the presence of nitrogenase (*nifH*) genes from heterotrophic N₂-fixing (diazotrophic) prokaryotes in unusual habitats challenge the paradigm that pelagic marine N₂ fixation is constrained to cyanobacteria in warm, oligotrophic, surface waters. Here, we compare NFR and diazotrophic diversity (assessed via high-throughput *nifH* sequencing) from a region known to be dominated by cyanobacterial diazotrophs (the North Pacific Subtropical Gyre, NPSG) to two regions dominated by heterotrophic diazotrophs: the Eastern South Pacific (ESP, from the Chilean upwelling system to the subtropical gyre) and the Pacific Northwest coastal upwelling system (PNW). We observed distinct biogeographical patterns among the three regions. Diazotrophic community structure differed strongly between the NPSG, dominated by cyanobacterium UCYN-A, and the ESP, dominated by heterotrophic *nifH* group 1J/1K, yet surface NFR were similar in magnitude (up to 5.1 nmol N L⁻¹ d⁻¹). However, while diverse, predominantly heterotrophic *nifH* genes were recovered from the PNW and the mesopelagic of the NPSG, NFR were undetectable in both of these environments (although glucose amendments stimulated low rates in the deep NPSG). Our work suggests that while diazotrophs may be nearly omnipresent in marine waters, the activity of this functional group is regionally restricted. Further, we show that the detection limits of the ¹⁵N₂ fixation assay suggest that many of the low NFR reported for the mesopelagic (often < 0.1 nmol N L⁻¹ d⁻¹ in the literature) are not indicative of active diazotrophy, highlighting the challenges of assessing the ecosystem significance of heterotrophic diazotrophs.

Nitrogen (N) availability limits phytoplankton production in most marine ecosystems (Gruber 2004), and thus partially determines the drawdown of inorganic carbon from the atmosphere. The oceanic reservoir of bioavailable N is largely controlled by the balance of specific microbial processes: dinitrogen (N₂) fixation adds fixed N and denitrification and anaerobic ammonia oxidation remove fixed N. Whether the global oceanic N budget is balanced or not is a topic of

longstanding controversy (see Galloway et al. 2004; Gruber 2004). Nevertheless, multiple lines of evidence suggest historical underestimations of both marine N₂ fixation rates (NFR) (Codispoti 2007; Deutsch et al. 2007; Großkopf et al. 2012) and the diversity and abundance of marine N₂-fixers (diazotrophs) (Riemann et al. 2010). These findings have driven a reassessment of N₂-fixing habitats and diazotrophic diversity (reviewed in Bombar et al. 2016).

N₂ fixation was traditionally thought to be dominated by cyanobacteria inhabiting warm, oligotrophic, surface ocean waters (Karl et al. 2002), but this paradigm is being challenged. Sequencing the *nifH* gene, which encodes the iron-protein component of the enzyme nitrogenase that catalyzes N₂ fixation, has revealed potential marine diazotrophs spanning diverse prokaryotic lineages (Zehr et al. 1998), and *nifH* amplicons from putative heterotrophs have been reported to outnumber cyanobacterial amplicons in global surface ocean waters (Riemann et al. 2010; Farnelid et al. 2011). Furthermore, heterotrophic *nifH* genes and transcripts have been recovered from environments previously unexplored for N₂

*Correspondence: rgradoville@coas.oregonstate.edu

^aPresent address: Ocean Sciences Department, University of California Santa Cruz, Santa Cruz, California

^bPresent address: Marine Biological Section, Department of Biology, University of Copenhagen, Helsingør, Denmark

Additional Supporting Information may be found in the online version of this article.

This is an open access article under the terms of the Creative Commons Attribution License, which permits use, distribution and reproduction in any medium, provided the original work is properly cited.

fixation, including coastal upwelling regimes, oxygen minimum zones, and the deep sea (Hewson et al. 2007; Sohm et al. 2011; Jayakumar et al. 2012). Active N_2 fixation in these environments, even at low rates, would increase overall marine N_2 fixation estimates and expand our understanding of the biogeographical patterns of an ecologically important functional group, the diazotrophs (e.g., Bonnet et al. 2013; Rahav et al. 2013).

The Eastern South Pacific (ESP), in particular, is a region that has garnered considerable attention as a potentially underappreciated habitat for marine N_2 fixation. Though historically understudied as an environment for diazotrophs (Luo et al. 2012), focus on the ESP increased after a numerical model predicted high NFR in the region (Deutsch et al. 2007). Despite model predictions, expeditions to the ESP have revealed low NFR in the oligotrophic gyre ($0.08\text{--}0.88\text{ nmol L}^{-1}\text{ d}^{-1}$, Halm et al. 2011; Dekaezemacker et al. 2013), albeit highly variable rates in the Chilean upwelling system ($0.1\text{--}127\text{ nmol L}^{-1}\text{ d}^{-1}$, Fernandez et al. 2011, 2015). The presence of inorganic N can suppress N_2 fixation by cyanobacterial diazotrophs (Knapp 2012; Knapp et al. 2012), so it is unsurprising that diazotrophic communities in the N-rich upwelling zone of the ESP appear to be heavily dominated by heterotrophic bacteria, particularly gamma-proteobacteria (Farnelid et al. 2011; Fernandez et al. 2011; Turk-Kubo et al. 2014). The quantitative Polymerase Chain Reaction (qPCR)-derived *nifH* abundances of select heterotrophic phylotypes, however, appear too low to account for even the low NFR observed to date (Turk-Kubo et al. 2014). This mismatch between proxies for cell abundances and rates implies an underestimation of diazotrophic abundance or cell-specific rates, and/or an overestimation of NFR. These findings point to significant concerns regarding the inaccuracy of historical NFR measurements (Mohr et al. 2010; Dabundo et al. 2014) that have since been partially addressed (Wilson et al. 2012; Böttjer et al. 2016) and, more importantly, highlight our incomplete knowledge of the physiology, biogeography, and ecology of heterotrophic diazotrophs.

In order to understand the linkage between the assembly of diazotrophic communities and the magnitude of NFR, we have developed a cross-ecosystem study spanning oligotrophic gyres to upwelling regimes. Specifically, we present the first pairing of NFR with fine-scale diazotrophic diversity assessments (via high-throughput *nifH* sequencing) in three oceanic regions: the ESP (from the upwelling zone to the gyre), the North Pacific Subtropical Gyre (NPSG), and the Pacific Northwest coast of the United States (PNW). While previous observations in the ESP indicate low NFR and cryptic heterotrophic diazotrophs, the NPSG fosters moderate NFR presumably driven by highly abundant cyanobacterial diazotrophs ($0.6\text{--}3.2\text{ nmol N L}^{-1}\text{ d}^{-1}$, Böttjer et al. 2016). Meanwhile, N_2 fixation has not been reported in the PNW, where the upwelling of cold, nitrate-rich waters would theoretically select against the growth of diazotrophs.

Comparisons of these three potential habitats enable a global biogeographical perspective of marine diazotrophy. Here, we also address discontinuities between the genetic potential for diazotrophy and the presence of detectable NFR.

Methods

Study sites and sampling strategy

Diazotrophic diversity and NFR were assessed in (1) the ESP (Center for Microbial Oceanography: Research and Education cruise aboard the R/V *Melville*, Biogeochemical Gradients: Role in Arranging Planktonic Assemblages [BIG RAPA], November to December 2010), (2) the Pacific Northwest California Current system (PNW, West Coast Ocean Acidification cruise aboard NOAA *Fairweather* and R/V *Point Sur*, August 2012, see Feely et al. 2013), and (3) at Station ALOHA (A Long Term Habitat Assessment) in the NPSG (Hawaiian Ocean Experiment Budget of Energy cruise aboard R/V *Kilo Moana*, March 2014) (Fig. 1). A summary of oceanographic sampling locations and conditions is provided in Table 1.

Water samples from all cruises were collected using sampling bottles attached to a CTD (conductivity, temperature, depth) rosette. In the ESP, N_2 fixation was assessed in surface waters (5 m), and diazotrophic diversity was assessed in surface and mesopelagic waters (5–420 m). NFR and diazotrophic diversity were assessed at depths targeting the surface mixed layer, oxycline, and oxygen minimum zone in the PNW, and at standard depths of 25 m (surface mixed layer), 75 m (\sim base of mixed layer), and 200 m (top of mesopelagic) in the NPSG.

Nitrogen fixation rates

NFR were assessed using a modification (Mohr et al. 2010; Wilson et al. 2012) of the original $^{15}N_2$ uptake method (Montoya et al. 1996) to avoid problems of bubble dissolution. $^{15}N_2$ gas (Cambridge Isotopes, 99%) was dissolved in degassed, filtered seawater. The $^{15}N_2$ content of this $^{15}N_2$ -enriched seawater was validated via Membrane Inlet Mass Spectrometry (MIMS), and the $^{15}N_2$ -enriched seawater was added to $^{15}N_2$ incubations (2–10% by volume, see Supporting Information). Purities of $^{15}N_2$ stocks were not assessed, although previous Cambridge Isotope $^{15}N_2$ batches have contained only trace contaminants of $^{15}NH_4^+$; at most this contamination is estimated to result in perceived NFR of $<0.02\text{ nmol N L}^{-1}\text{ d}^{-1}$ (Dabundo et al. 2014).

Before NFR sampling, all bottles were thoroughly acid-washed and milli-Q rinsed; bottles were also rinsed with water from the target collection depth three times before filling. These steps were intended to minimize potential trace metal contamination. For sampling, duplicate or triplicate polycarbonate bottles (1.1–4.5 L) were filled to capacity, avoiding air contamination, and capped with septa closures. Samples were spiked with $^{15}N_2$ enriched seawater and incubated on deck for 24 h at approximately in situ temperature, either in the dark or with screening to mimic approximate in situ light

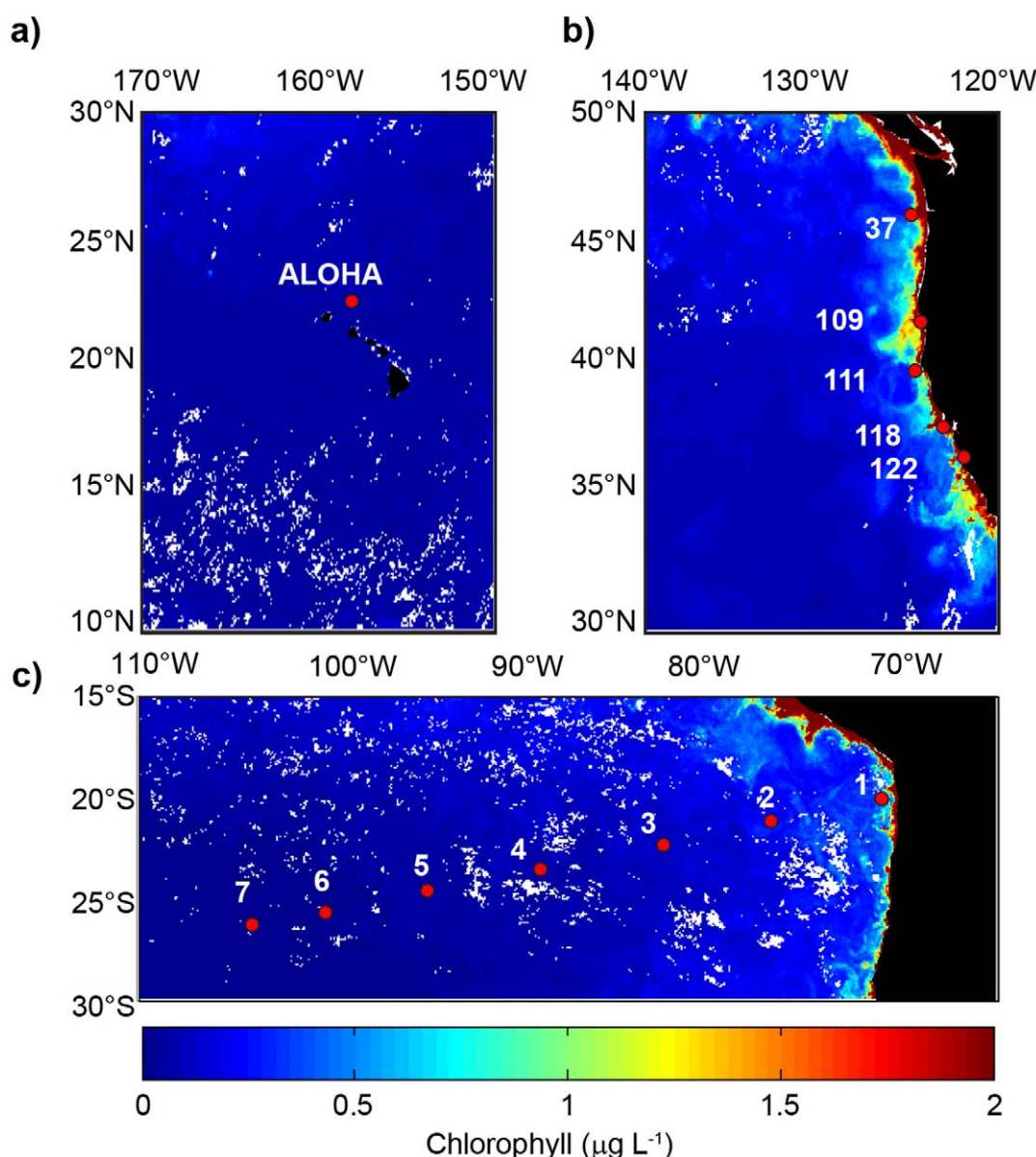


Fig. 1. Location of sampling stations from the North Pacific Subtropical Gyre (NPSG, **a**), Pacific Northwest (PNW, **b**), and Eastern South Pacific (ESP, **c**) cruises. Stations are superimposed onto surface chlorophyll concentrations obtained from 9 km-binned MODIS satellite data (<http://oceandata.sci.gsfc.nasa.gov/>) from the month sampled (March 2014 for NPSG, August 2013 for PNW, and November 2010 for ESP).

conditions (Table S1, see Supporting Information for a more detailed description of $^{15}\text{N}_2$ incubations). Incubations were terminated by gentle filtration of suspended material onto 25 mm diameter pre-combusted GF/F filters. Additionally, time-zero samples (the natural abundance of $\delta^{15}\text{N}$ of suspended particulate N) were collected at each time point and depth. Filters were frozen at -80°C and shipped to Oregon State University, where they were dried at 60°C overnight and packed into tin and silver capsules. Isotopic composition and masses of particulate N and C were measured with an isotope ratio mass spectrometer at the University of California Davis

Stable Isotope Facility, or at Oregon State University. NFR were calculated according to Montoya et al. (1996) with the modification that rates are expressed as $\text{nmol N L}^{-1} \text{d}^{-1}$ rather than $\text{nmol N}_2 \text{L}^{-1} \text{d}^{-1}$.

Diazotrophic diversity

On all cruises, seawater for DNA was collected in 1–4 L acid-washed, milliQ-rinsed polycarbonate bottles and gently filtered onto 25 mm $0.2 \mu\text{m}$ Supor membranes (Pall Corporation). Filters from PNW and NPSG cruises were stored at -20°C or -80°C until extraction using the DNeasy Plant

Table 1. Regional summary and environmental conditions of sampling stations on North Pacific Subtropical Gyre (NPSG), Eastern South Pacific (ESP), and Pacific Northwest (PNW) cruises. Sea surface temperature (SST, °C) and chlorophyll fluorescence (Chl, $\mu\text{g L}^{-1}$) were measured using conductivity–temperature–depth sensors (excluding PNW Chl, which were measured fluorometrically). Nitrate + nitrite (N + N, $\mu\text{mol kg}^{-1}$) and phosphate (PO_4 , $\mu\text{mol kg}^{-1}$) concentrations were measured with discrete bottle samples taken at ~ 5 m depth. ND indicates no data available.

Region	Summary	Station	Date	Location	SST	N+N	PO_4	Chl
NPSG	Occupation at Stn. ALOHA in the NPSG. N_2 fixation rates and <i>nifH</i> diversity assessed at 25 m, 75 m, and 200 m	ALOHA	12 Mar 14	22°46.1'N, 157°59.7'W	24.2	ND	ND	0.16
		ALOHA	15 Mar 14	22°46.8'N, 158°5.1'W	24.3	0.01	0.09	0.17
		ALOHA	17 Mar 14	22°44.5'N, 158°5.9'W	23.9	0.02	0.08	0.28
		ALOHA	18 Mar 14	22°46.5'N, 158°4.9'W	23.8	ND	ND	0.25
		ALOHA	19 Mar 14	22°46.7'N, 158°4.9'W	23.9	0.01	0.11	0.23
		ALOHA	21 Mar 14	22°46.7'N, 158°5.0'W	23.8	0.02	0.11	0.21
ESP	Transit from the nutrient-rich, productive Chilean upwelling system (Stn. 1) to the low-nutrient, low-chlorophyll gyre (Stn. 7). N_2 fixation measured at 5 m only; <i>nifH</i> diversity measured from 5 m to 420 m	1	21 Nov 10	20° 4.8'S, 70°48.0'W	18.9	0.44	0.88	0.83
		2	25 Nov 10	21°10.8'S, 76°57.0'W	17.9	0.25	0.48	0.53
		3	28 Nov 10	22°15.6'S, 82°21.0'W	17.9	0.23	0.45	0.20
		4	01 Dec 10	23°27.6' S, 88°45.6'W	18.7	ND	ND	0.24
		5	05 Dec 10	24°33.6'S, 94°43.2'W	19.7	ND	ND	0.11
		6	07 Dec 10	25°33.0'S, 100°8.4'W	20.7	ND	ND	0.06
		7	09 Dec 10	26°15.0'S, 103°57.6'W	21.5	0.27	0.21	0.07
PNW	Coastal cruise sampling continental slope and shelf stations in the productive California Current upwelling system. N_2 fixation (Stn. 37, 109, 118 only) and <i>nifH</i> diversity assessed from 3 m to 700 m at depths targeting surface, oxycline, and oxygen minima	37	09 Aug 13	46°7.2'N, −124°54.6'W	15.8	0.07	0.31	0.19
		109	23 Aug 13	41°58.2'N, −124°24.0'W	10.8	16.86	1.39	ND
		111	24 Aug 13	40°6.0'N, −124°42.6'W	11.9	9.23	1.00	ND
		118	27 Aug 13	37°52.2'N, −123°3.6'W	14.8	0.50	0.32	ND
		122	28 Aug 13	36°43.8'N, −121°58.2'W	14.9	0.06	0.36	ND

MiniKit (Qiagen) following manufacturer's instructions, with modifications to include freeze-thaw and proteinase K treatment for additional cell disruption. On the ESP cruise, water was size-fractionated, and DNA samples (0.2–10 μm fraction only) were transferred into sterile bead beating tubes containing a 1 : 1 mixture of 0.1 mm and 0.5 mm glass beads (BioSpec Products), flash-frozen, and stored at -80°C until extraction. All ESP DNA extractions, qPCR and PCR reactions were carried out as described by Turk-Kubo et al. (2012) (see Supporting Information). DNA concentrations were measured with PicoGreen using a MicroMax 384 plate reading fluorometer, and extracts were stored at -20°C or -80°C .

The polymerase chain reaction (PCR) was used to amplify *nifH* genes for all samples using nested degenerate *nifH* primers (Zehr and McReynolds 1989; Zani et al. 2000). PCRs were performed using a Veriti thermocycler (Applied Biosystems) with 10 μL or 20 μL reaction volumes. The first round of PCR contained 1X PCR buffer, 200 $\mu\text{mol L}^{-1}$ dNTPs, 3% BSA, 4 mmol L^{-1} Mg^{2+} , 0.1U Platinum High Fidelity *Taq* polymerase (Invitrogen), 1 μL DNA, and 1 $\mu\text{mol L}^{-1}$ *nifH1* and *nifH2* primers (Zehr and McReynolds 1989). This reaction was cycled at 94°C for 7 min, then 30 cycles of 94°C for 1 min, 57°C for 1

min, and 72°C for 1 min, and finally 72°C for 7 min. The second round of *nifH* PCR used the same thermocycling conditions (except for a 5 min initial denaturation step) and components, but used 1 μL PCR product from the first reaction and custom primers comprised of gene-specific sites, dual-indexed barcodes, Illumina linkers, and a sequencing primer binding region, similar to those described by Kozich et al. (2013) (Supporting Information Table S2). Triplicate PCR products were visualized by gel electrophoresis, pooled, and quantified as above. Only samples with three successful PCR reactions were included for sequencing, and negative controls and filter blanks were sequenced despite the absence of visual bands after amplification. Amplicons were pooled at equal concentrations, cleaned using the UltraClean PCR (MoBio) and AMPure XP Bead cleanup kits, and sequenced using MiSeq Standard v.3, 2×300 bp paired-end sequencing at Oregon State University.

Sequence reads were demultiplexed using the Illumina MiSeq Reporter (MSR) version 2.5.1. Forward and reverse barcodes were used for demultiplexing; however, due to poor quality of reverse reads, only forward reads were used for phylogenetic analyses. Quality control was performed

using Mothur (Schloss et al. 2009), discarding reads with ambiguities, poor quality (average score < 25 or any score < 20), or homopolymers (> 8 bp). Forward primers were removed, and all sequences were trimmed to 213 bp. Operational taxonomic units (OTUs) were clustered at 97% nucleotide sequence similarity, and a de novo chimera check was performed using Usearch (Edgar 2010). OTUs containing chimeras, frameshifts, and non-*nifH* sequences were removed, and sequences were subsampled to 10,386 sequences per sample.

Translated OTUs were classified into canonical *nifH* gene clusters (Zehr et al. 2003b) using BLAST-p similarity to a reference database of *nifH* sequences previously assigned to *nifH* groups (<http://www.jzehrlab.com/#!/nifh-database/c1coj>). Sequences with < 90% amino acid similarity to any reference sequence or equal similarity to sequences from multiple *nifH* groups are termed “undefined.” Shannon diversity calculations and nonmetric multidimensional scaling analyses (Bray–Curtis similarity) were performed using QIIME (Caporaso et al. 2010). Sequences are available from NCBI (accession SRP078449).

Diazotrophic quantification

Droplet digital PCR (ddPCR) was used to quantify *nifH* copies from UCYN-A in NPSG samples and alpha-HQ586648 in ESP samples. Droplet digital PCR was performed using the Bio-Rad QX200 system. Diluted DNA extracts were used as templates in assays designed to amplify *nifH* genes from UCYN-A and alpha-HQ586648. Primer/probe sets were slightly modified from those described by Church et al. (2005a) (forward primer: GGCTATAACAACGTTTTATGCGTTGA, reverse primer: ACCACGACCAGCACATCCA, probe: TCCGGTGGTCTGAGCCTGGA) and Zhang et al. (2011) (forward primer: ATCACCGCCATCAACTTCCT, reverse primer: AGACCACGTGCCCCAGAAC, probe: CGCCTACGATGACGTGGATTACGTGTCC) to minimize mismatches with sequences from OTU 1 (UCYN-A) and OTU 2 (alpha-HQ586648). Reactions consisted of 10 μ L PCR mastermix (Bio-Rad), 900 nM primers, 250 nM probes, and ~ 1–50 ng DNA. Droplet generation, PCR, and scanning were conducted at the Oregon State University Center for Genome Research and Biocomputing according to manufacturer instructions (Bio-Rad), with an annealing temperature of 57°C. Standard curves were not used for these assays as ddPCR produces absolute concentrations without the need for standards. No template controls (NTC) were included in the ddPCR run; no UCYN-A or alpha-HQ586648 gene copies were detected in any of the 6 NTC samples. Data were analyzed using the QuantaSoft analysis software package.

Statistical methods

Simple linear regressions and one-way ANOVA with subsequent Tukey Honest Significance Difference (HSD) tests of multiple comparisons were performed using the program R (<http://www.r-project.org/>). Significant differences in community structure among regions were tested using a one-way

ANOSIM in PRIMER. A sensitivity analysis for NFR measurements was performed as described by Montoya et al. (1996). The minimum quantifiable rate for each water mass was calculated using standard propagation of errors via the observed variability between replicate samples (Supporting Information Table S3; region-averaged values provided in Table 2). We also used the approach of Montoya et al. (1996) to calculate an alternative detection limit by setting $[A_{\text{PNf}} - A_{\text{PN0}}]$ equal to 0.00146 atom %.

Results

Oceanographic conditions

Samples used for this study came from diverse hydrographic and biogeochemical regions (Fig. 1; Table 1). The ESP cruise transited through a biogeochemical gradient from highly productive, upwelling-influenced waters on the Chilean shelf to warmer, stratified, oligotrophic stations in the South Pacific gyre (Rii et al. 2016). The PNW cruise transited through continental shelf and slope stations in the Northern California Current system during the summer upwelling season. The NPSG cruise was conducted at Station ALOHA in oligotrophic conditions (Table 1).

Nitrogen fixation rates

NFR varied by region and by depth (Fig. 2). On the ESP transit cruise, surface NFR were highest near the coast (5.1 nmol N L⁻¹ d⁻¹ at Stn. 1), and decreased across the westward transit, with the lowest rates in the gyre (0.46 nmol N L⁻¹ d⁻¹ at Stn. 7) (Fig. 2). All rates exceeded the minimum quantifiable rate, defined here as the propagated error for each measurement, which ranged from 0.15 to 0.77 nmol N L⁻¹ d⁻¹ (Supporting Information Table S3). Subsurface NFR were not assessed in the ESP.

In the NPSG, we measured rates of 2.5–3.9 nmol N L⁻¹ d⁻¹ at 25 m and 0.4–1.9 nmol N L⁻¹ d⁻¹ at 75 m. N₂ fixation was undetectable at 200 m under ambient conditions, though amendment with 3 μ mol L⁻¹ glucose stimulated rates of 0.1–0.3 nmol N L⁻¹ d⁻¹; these rates exceeded the minimum quantifiable rate, which ranged from 0.04–1.08 nmol N L⁻¹ d⁻¹ for the region (Supporting Information Table S3).

N₂ fixation was not detected at any station or depth on the PNW cruise. Most measurements fell below the minimum quantifiable rate, which ranged from 0.06 to 0.69 nmol N L⁻¹ d⁻¹ (Fig. 2; Supporting Information Table S3). Two measurements were above the minimum quantifiable rate but below the alternate limit of detection suggested by Montoya et al. (1996) (calculated by setting $[A_{\text{PNf}} - A_{\text{PN0}}]$ equal to 0.00146 atom %, Supporting Information Table S3) and are thus regarded as not detected.

Diazotrophic diversity

Diazotrophic diversity was assessed via high-throughput sequencing of partial *nifH* gene sequences. Only samples with three successful PCR amplifications (achieved for 18/21

Table 2. Cruise-averaged sensitivity analysis for N₂ fixation rate (NFR) measurements.*

Cruise	Parameter (X)	Value	SD	$\delta\text{NFR}/\delta X$	Error contribution (SD \times [$\delta\text{NFR}/\delta X$]) ²	% Total error	Summary
ESP	Δt	1.00	1.94×10^{-17}	-1.17×10^{-1}	1.76×10^{-33}	0.00	
	A_{N_2}	4.35%	5.10×10^{-3}	-4.21×10^1	7.58×10^{-2}	27.3	Mean.....1.81 nmol N L ⁻¹ d ⁻¹
	A_{PN_0}	0.366%	3.24×10^{-6}	-3.22×10^4	3.59×10^{-2}	11.3	MQR.....0.40 nmol N L ⁻¹ d ⁻¹
	A_{PNf}	0.371%	7.18×10^{-6}	3.22×10^4	2.61×10^{-2}	19.9	LOD.....0.47 nmol N L ⁻¹ d ⁻¹
	$[\text{PN}]_f$	1.25×10^3	1.71×10^2	1.35×10^{-3}	5.60×10^{-2}	41.5	HET-MQR..... 9.7×10^4 cells L ⁻¹
NPSG	Δt	1.06	5.58×10^{-3}	-1.23×10^0	5.75×10^{-5}	0.02	
	A_{N_2}	2.57%	1.16×10^{-3}	-57.9×10^1	1.37×10^{-2}	5.31	Mean.....1.32 nmol N L ⁻¹ d ⁻¹
	A_{PN_0}	0.372%	1.68×10^{-5}	1.40×10^4	1.13×10^{-1}	60.5	MQR.....0.39 nmol N L ⁻¹ d ⁻¹
	A_{PNf}	0.378%	1.28×10^{-5}	1.41×10^4	1.10×10^{-1}	30.6	LOD.....0.21 nmol N L ⁻¹ d ⁻¹
	$[\text{PN}]_f$	3.24×10^2	23.1×10^1	2.88×10^{-3}	1.14×10^{-2}	3.65	HET-MQR..... 9.5×10^4 cells L ⁻¹
PNW	Δt	1.05	8.02×10^{-3}	4.10×10^{-2}	3.55×10^{-5}	0.01	
	A_{N_2}	3.26%	3.82×10^{-3}	1.18×10^{-2}	2.50×10^{-3}	3.68	Mean.....0 nmol N L ⁻¹ d ⁻¹
	A_{PN_0}	0.370%	1.89×10^{-6}	-7.44×10^2	3.50×10^{-2}	38.6	MQR.....0.27 nmol N L ⁻¹ d ⁻¹
	A_{PNf}	0.370%	3.24×10^{-6}	7.44×10^2	8.81×10^{-2}	44.9	LOD.....1.09 nmol N L ⁻¹ d ⁻¹
	$[\text{PN}]_f$	2.30×10^3	2.00×10^2	-7.10×10^{-6}	2.65×10^{-3}	12.8	HET-MQR..... 6.6×10^4 cells L ⁻¹

* The contribution of each source of error to the total uncertainty is provided, as performed by Montoya et al. (1996) using standard methods for error propagation. A_{N_2} , A_{PN_0} , and A_{PNf} represent the initial atom % ¹⁵N₂ gas, initial atom % ¹⁵N of PN, and final atom % ¹⁵N of PN, respectively. $[\text{PN}]_f$ represents the final concentration of N (nmol N L⁻¹), and Δt represents the incubation time (days). The third and fourth columns represent the observed average and standard deviation (SD) for each measured parameter from duplicate or triplicate incubation bottles. The fifth column represents the partial derivative of the NFR with respect to each parameter, evaluated using the provided average and SD. The sixth and seventh columns represent the absolute and relative error associated with each parameter. The total uncertainty associated with each measurement is termed the “Minimal Quantifiable Rate” (MQR). An alternative limit of detection (LOD) was calculated by setting $[A_{\text{PNf}} - A_{\text{PN}_0}]$ equal to 0.00146 atom %, as described by Montoya et al. (1996). HET-MQR represents a minimal heterotrophic diazotrophic cell concentration required to produce the MQR, calculated using the highest cell-specific NFR reported by Bentzon-Tilia et al. (2015) for the alpha-proteobacterial isolate *R. palustris* BAL398 (0.52 fmol C₂H₄ cell⁻¹ h⁻¹; ~ 4.1 fmol N cell⁻¹ d⁻¹). Note that all values here represent regional averages; see Supporting Information Table S3 for the full sensitivity analysis.

NPSG samples, 20/23 ESP samples, and 12/13 PNW samples) and sufficient reads to subsample down to 10,386 sequences per sample were retained ($n = 49$ samples). Rarefaction analyses show that our sequencing effort was sufficient to fully assess *nifH* diversity from most samples (Supporting Information Fig. S1). The subsampled datasets were used for all downstream analyses (excluding Supporting Information Figs. S1 and S2).

To test for the possibility of contaminant sequences from PCR reagents or other sample processing procedures (Zehr et al. 2003a), representative sequences from each OTU were aligned against known contaminant *nifH* sequences. Four OTUs had >95% nucleotide identity to known contaminants; the majority of these sequences were from ESP samples (Supporting Information Table S4). None of the negative control samples contained *nifH* sequences; however, two of four triplicate-pooled filter blank samples contained a small number of sequences (1574 and 634) (Fig. S2, see Supporting Information).

Clustering sequences at 97% nucleotide similarity yielded 201 OTUs; 150 of these (> 99% of total sequences) passed

quality control procedures and were used for analyses. All OTUs clustered with *nifH* sequences from Clades I and III, and most were associated with group 1J/1K (alpha- and beta-proteobacteria) and 1B (cyanobacteria) (Figs. 3, 4). Diazotrophic community structure differed strongly between regions (Global ANOSIM $R = 0.87$, $p = 0.001$) (Fig. 5). Likewise, the regions were dominated by different diazotrophic taxa (Fig. 4) and contained few shared OTUs (Fig. 3).

In the NPSG, most *nifH* sequences were classified as cyanobacteria (Fig. 4). 66.7% of NPSG sequences grouped with sequences from the cyanobacterium UCYN-A (Figs. 3, 4, Supporting Information Fig. S3); lower limit concentrations of the most abundant UCYN-A phylotype (OTU 1, 55.8% of NPSG sequences) ranged from 3.3×10^4 to 4.4×10^5 *nifH* copies L⁻¹ in 25 m and 75 m water (Supporting Information Table S5). Other prominent cyanobacterial phylotypes grouped with *Trichodesmium* (~ 4.8% of NPSG sequences), and < 0.1% of NPSG sequences were closely related to *Richelia*, *Crocospaera*, and unidentified cyanobacteria sharing < 94% nucleotide similarity to cultured representatives. Other than cyanobacteria, 20.6% of NPSG sequences were assigned to the gamma-

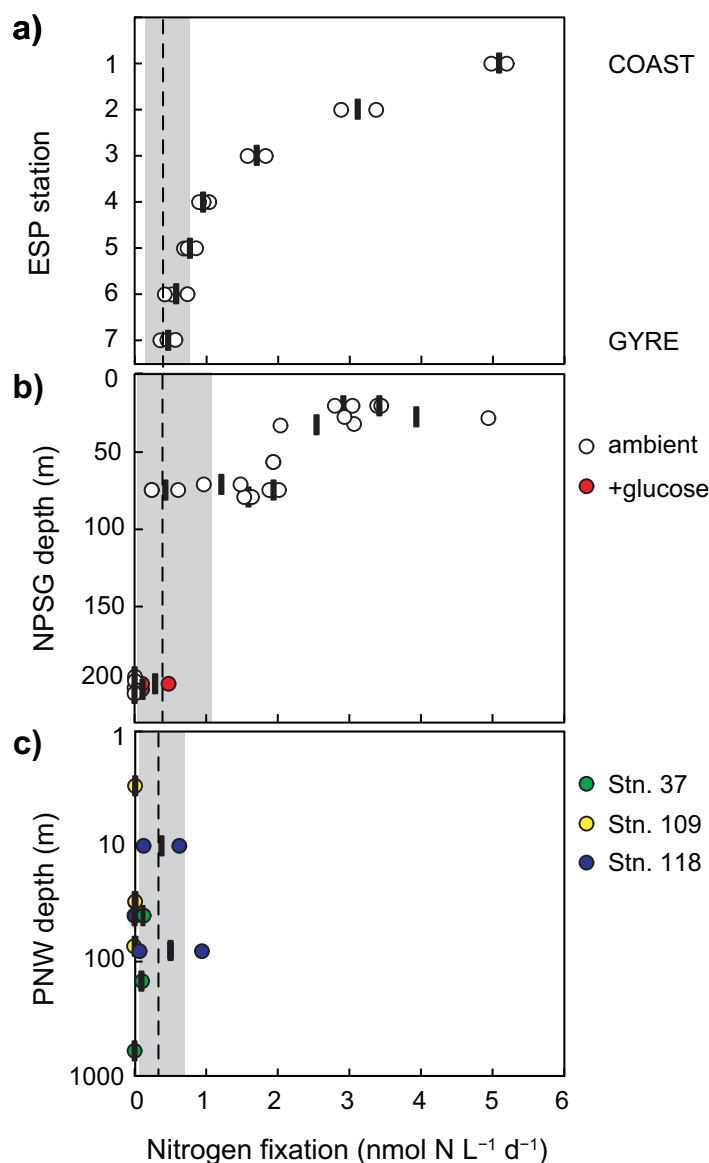


Fig. 2. Nitrogen fixation rates (NFR) on Eastern South Pacific (ESP, **a**), North Pacific Subtropical Gyre (NPSG, **b**), and Pacific Northwest (PNW, **c**) cruises, measured via the $^{15}\text{N}_2$ assimilation assay. Note that NFR at ESP stations were only measured in surface waters. Circles represent individual measurements and vertical dashes represent averages. Colors denote glucose amendment (**b**) or station (**c**). Black dashed lines represent cruise-averaged minimum quantifiable rates, with the full range of minimum quantifiable rates observed on each cruise (Supporting Information Table S3) indicated by gray shading. N_2 fixation rates below the cruise-minimum minimum quantifiable rate were moved to zero.

proteobacterial group 1G (Fig. 4). These sequences are dominated by OTU 3, which matches with qPCR primer/probe sets designed to amplify the group “Gamma A” (Church et al. 2005a; Moisaner et al. 2008; Langlois et al. 2015). Together, cyanobacteria and group 1G represent $>99\%$ of sequences from 25 m and 75 m samples. While *nifH* genes were successfully amplified from all 25 m and 75 m samples, triplicate

PCRs were successful for only 3/6 of the 200 m samples; dominant taxa and OTUs were less consistent among these samples (Fig. 4, Supporting Information Fig. S3).

Heterotrophs dominated the diazotrophic community in the $<10\ \mu\text{m}$ size fraction of ESP samples (Fig. 4). Most sequences were assigned to group 1J/1K, and $<0.2\%$ of sequences were assigned to cyanobacteria. Five OTUs (2, 4, 5, 10, and 16), comprising $>90\%$ of total ESP sequences (Supporting Information Fig. S3), were tested in silico against published qPCR primer/probe sets targeting heterotrophic marine diazotrophs. OTU 2 matched the alpha-HQ586648 forward primer designed by Zhang et al. (2011) (probe and reverse primers were beyond the range of our partial *nifH* sequences, Supporting Information Table S6); lower-limit abundance estimates of alpha-HQ586648 ranged from 1.5×10^2 to 4.4×10^3 *nifH* copies L^{-1} (Supporting Information Table S5). OTUs 4, 5, 10, and 16 did not match existing primer/probe sets (Supporting Information Table S6). Diazotrophic diversity in the ESP was not assessed for the $>10\ \mu\text{m}$ size fraction, which may have biased against the recovery of *nifH* genes from large or particle-associated diazotrophs.

Diazotrophic community composition from PNW samples was highly variable among stations and depths. The majority of PNW sequences clustered with heterotrophic taxa, though a sample from 150 m at Stn. 37 was dominated by UCYN-A sequences (Fig. 4). Overall, the most abundant *nifH* group was 1J/1K, which constituted 40.4% of total PNW sequences. However, a substantial fraction of PNW sequences were also assigned to groups 1A (delta-proteobacteria), 1G (gamma-proteobacteria), 1O/1P (beta-, gamma-proteobacteria), and group III (anaerobic delta-proteobacteria) (Fig. 4). Unlike the ESP and NPSG, very few OTUs were dominant in more than one sample (Supporting Information Fig. S3).

Alpha diversity metrics were calculated using the *nifH* sequence dataset. Shannon diversity was significantly higher in the PNW (Tukey HST $p=0.004$) and the NPSG (Tukey HST $p=0.015$) than in the ESP (Fig. 6). There was a negative relationship between Shannon diversity and NFR in the NPSG (linear regression, $R^2=0.316$, $p=0.015$) but no significant relationship in the ESP ($p>0.05$, Supporting Information Table S7). There were no significant relationships between Shannon diversity and temperature, oxygen concentration, or nitrate concentration (linear regression, $p>0.05$, Supporting Information Table S7).

Discussion

Cosmopolitan diazotrophs with taxa-specific biogeography

Increasing reports of heterotrophic diazotrophs in “unusual” environments have challenged the common assumption that marine N_2 fixation is dominated by cyanobacteria that inhabit warm, N-limiting waters (Bombar et al. 2016). Here, we probed for *nifH* genes in three regions: the

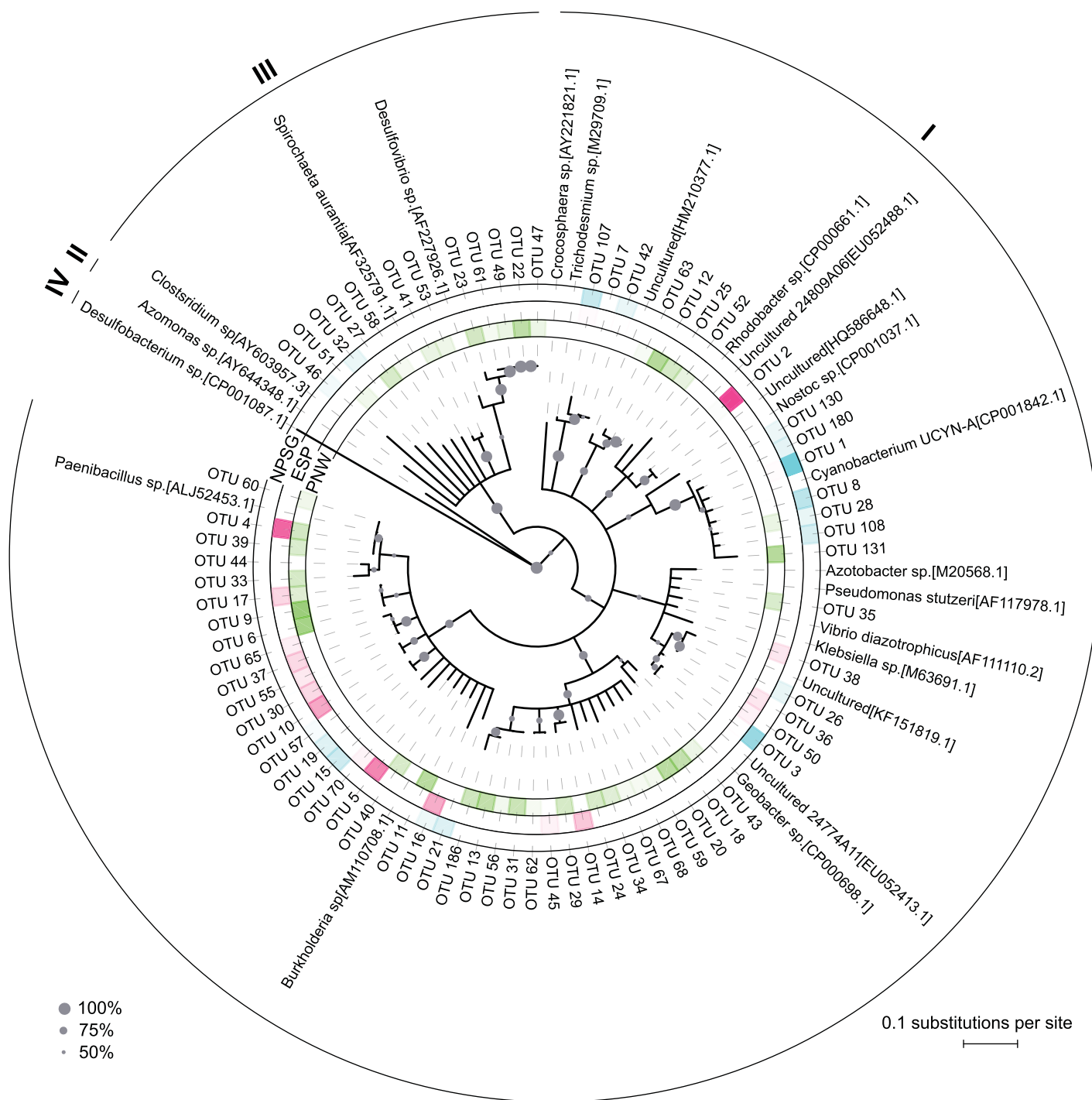


Fig. 3. Neighbor-joining phylogenetic tree derived from partial *nifH* amino acid sequences from North Pacific Subtropical Gyre (NPSG), Eastern South Pacific (ESP), and Pacific Northwest (PNW) cruises. Representative sequences from each operational taxonomic unit (OTU) containing > 10 sequences in the rarefied dataset (71 OTUs representing > 99% of total sequences) are displayed on the tree. Colored bars represent the log-transformed relative abundances of OTUs from the NPSG (blue), PNW (green), and ESP (red) samples, with darker shading indicating higher relative abundance. Bootstrap values (1000 replicates) of > 50% are represented in the tree with size-proportional gray circles. The taxonomic affiliations of OTUs with canonical *nifH* clades (Zehr et al. 2003) are displayed in roman numerals. An alignment of the sequences represented in this tree is provided in Supporting Information Fig. S4. Tree was produced using the Interactive Tree of Life (<http://itol.embl.de/>, Letunic and Bork 2016).

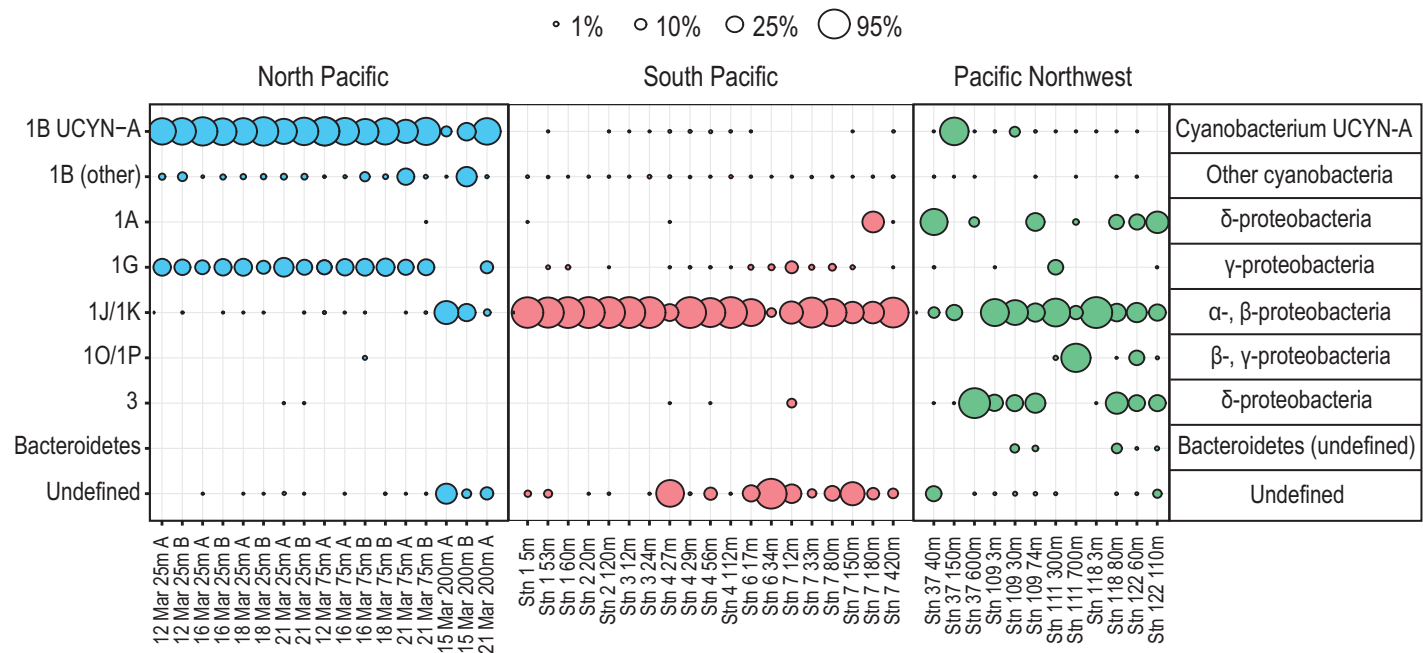


Fig. 4. Percentages of sequences from North Pacific Subtropical Gyre (blue), Eastern South Pacific (red), and Pacific Northwest (green) samples assigned to *nifH* gene cluster groups. Representative taxa within each *nifH* group are provided to the right. Group 1B was divided into “UCYN-A” and “other cyanobacteria.” Sequences with < 90% amino acid similarity to reference sequences or equal similarity to multiple reference sequences defined to different *nifH* clusters are termed “Undefined.”

NPSG, considered a classical habitat for diazotrophs, the ESP, where the functionally important diazotrophs appear cryptic (Turk-Kubo et al. 2014), and the PNW, where diazotrophy would not be expected. We observed the genetic potential for diazotrophy in all environments assessed, including the cold, N-rich waters of the PNW. Our data show strong differences in diazotrophic community structure between regions, implying distinct biogeography for these organisms.

The first global high-throughput *nifH* sequencing effort by Farnelid et al. (2011) reported heterotrophic diazotrophs outnumbering cyanobacteria in all regions assessed, including one sample from the NPSG. In contrast, cyanobacteria dominated our *nifH* sequences in all 14 NPSG euphotic zone samples (Fig. 4). In agreement with previous studies at Stn. ALOHA using qPCR and *nifH* clone libraries (Church et al. 2005a, 2008; Böttjer et al. 2014), we found that the cyanobacterium UCYN-A was present at high concentrations (10^4 – 10^5 *nifH* copies L^{-1}) and dominated the diazotrophic community in the euphotic zone (Fig. 4; Supporting Information Table S5). We also observed a large proportion of euphotic zone *nifH* sequences associated with Gamma A, a globally distributed group of marine gamma-proteobacteria that has been previously detected at Stn. ALOHA (Church et al. 2005a; Langlois et al. 2015).

In contrast to the NPSG, the ESP diazotrophic community appears dominated by heterotrophs, a finding which agrees with previous studies (Halm et al. 2011; Turk-Kubo et al. 2014). However, while Halm et al. (2011) and Turk-Kubo

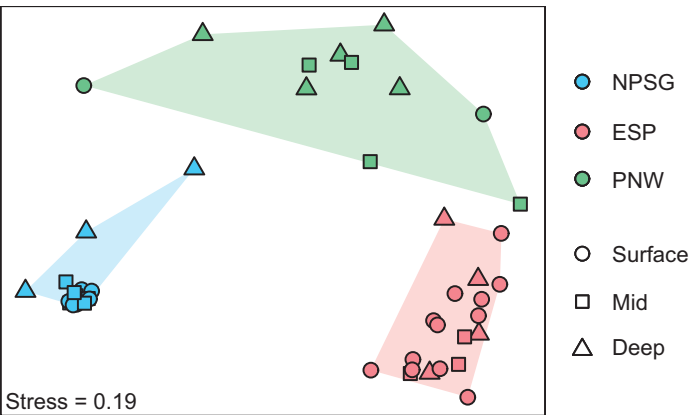


Fig. 5. Non-metric multi-dimensional scaling (NMDS) plot derived from the Bray-Curtis dissimilarity matrix of *nifH* OTUs from North Pacific Subtropical Gyre (NPSG), Eastern South Pacific (ESP), and Pacific Northwest (PNW) cruises. Each point represents an individual sample. Definition of depth classes vary by cruise: “Surface” indicates 25 m (NPSG), above the deep chlorophyll maxima (DCM, ESP), or the oxygen maxima (PNW), “Mid” indicates 75 m (NPSG), ~ DCM (ESP), or the oxycline (PNW), and “Deep” indicates 200 m (NPSG), below the DCM (ESP), or the oxygen minima (PNW).

et al. (2014) reported gamma-proteobacterial dominance, the majority of our sequences grouped with 1J/1K (alpha- and beta-proteobacteria), and the gamma-proteobacterial phylo- types previously quantified in the ESP were not dominant in

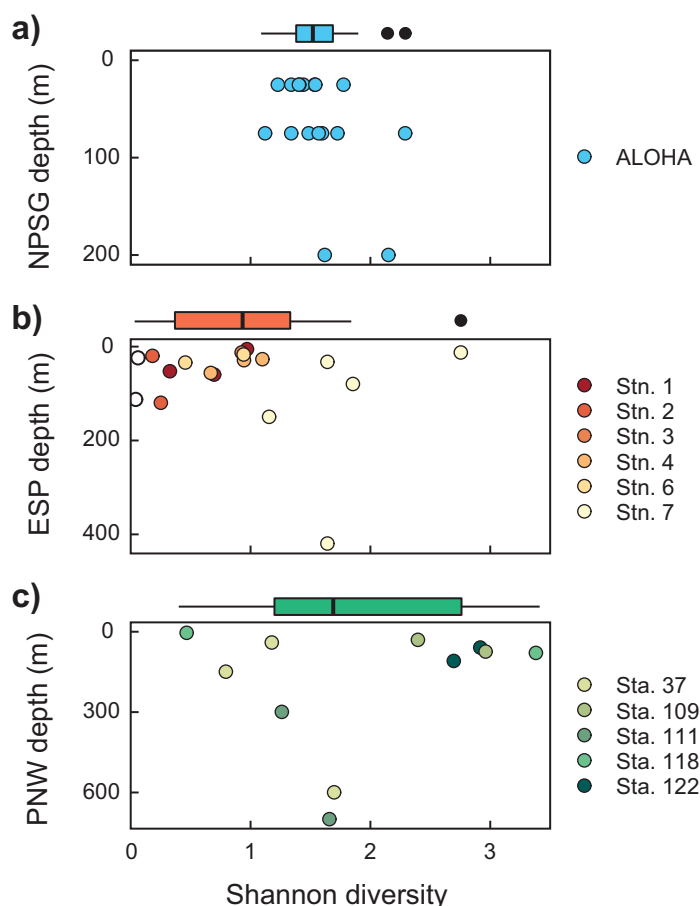


Fig. 6. Estimates of Shannon diversity for North Pacific Subtropical Gyre (a), Eastern South Pacific (b), and Pacific Northwest (c) cruises. Boxplots above each panel represent the depth- and station-pooled Shannon diversity from each cruise. Values are derived from partial *nifH* DNA sequences (clustered into 97% OTUs).

our dataset (Fig. 4; Supporting Information Table S6). It is possible that using only the $<10\ \mu\text{m}$ size fraction for ESP samples introduced bias by excluding particle-associated heterotrophs or large cyanobacterial cells. However, the absence of diatoms known to harbor diazotrophic cyanobacterial symbionts in a 16S rRNA plastid dataset obtained on the same cruise (Rii pers. comm.) and our poor success in qPCR assays targeting gamma-proteobacteria using all DNA size fractions (data not shown) lead us to conclude that the 1J/1K group was likely dominant.

Perhaps the most striking feature in the ESP is the consistency of dominant diazotrophic taxa and phylotypes among stations and depths (Fig. 4; Supporting Information Fig. S3). This homogeneity is quite surprising considering the strong biogeochemical gradients in temperature, nutrients and chlorophyll across the Chilean upwelling zone into the South Pacific gyre. In particular, OTU 2 was the most abundant phylotype in both the gyre and coastal stations (Supporting Information Fig. S3), and also matches *nifH*

sequences previously recovered from the Peruvian upwelling system, the Indian ocean, and the South China Sea (Fernandez et al. 2011; Zhang et al. 2011; Shiozaki et al. 2014). This finding counters previous observations of few heterotrophic diazotrophs with basin-wide distributions (Turk-Kubo et al. 2014). At present we do not have an explanation for the observed homogeneity of diazotrophic phylotypes along this oceanographic transect; further studies are needed to explore the stability of diazotrophic assemblages in this region in response to environmental perturbations.

While our deep-sequencing effort in the ESP and NPSG euphotic zone provides a higher resolution examination of diazotrophic diversity in previously explored regions, to our knowledge, our study is the first to recover *nifH* genes from PNW and mesopelagic NPSG waters. PNW samples were dominated by diverse heterotrophic taxa, while mesopelagic NPSG samples contained relatively abundant cyanobacteria and heterotrophs, perhaps originating from sinking organic particles (Figs. 3, 4). Both of these regions had highly dissimilar diazotrophic communities among samples compared to samples from the NPSG euphotic zone and the ESP (Fig. 5). Our findings add to the growing literature reporting diazotrophic genes in deep, dark, and N-rich environments.

Mixed evidence for nitrogen fixation in “unusual” environments

Marine N_2 fixation is typically facultative and regulated by physiological and environmental constraints (Paerl et al. 1987); thus, the presence of heterotrophic diazotrophs does not indicate active NFR. Yet recent studies have reported not only the presence of *nifH* genes, but also active N_2 fixation in aphotic, N-rich waters, and it has been suggested that these depth-integrated rates could have a significant impact on the marine N budget (Bonnet et al. 2013). While mesopelagic NFR are low (typically $\leq 0.5\ \text{nmol N L}^{-1}\ \text{d}^{-1}$ and often $\leq 0.1\ \text{nmol N L}^{-1}\ \text{d}^{-1}$, e.g., Bonnet et al. 2013; Rahav et al. 2013), the absence of any detectable N_2 fixation is rarely reported. Here, we tested for N_2 fixation at coastal PNW stations encompassing a range of temperature, nitrate, and oxygen concentrations (Table 1, Supporting Information Table S1). We observed no measurable NFR. Likewise, we observed no measurable NFR in 200 m NPSG samples under ambient conditions, though $3\ \mu\text{mol L}^{-1}$ glucose amendments stimulated low rates (Fig. 2).

The absence of detectable NFR in the PNW and mesopelagic NPSG samples is not surprising when considering the sensitivity of the $^{15}\text{N}_2$ assay. Our minimum quantifiable rates ranged from $0.06\text{--}0.69\ \text{nmol N L}^{-1}\ \text{d}^{-1}$ and $0.04\text{--}0.12\ \text{nmol N L}^{-1}\ \text{d}^{-1}$ for PNW and 200 m NPSG samples, respectively, and thus preclude the detection of NFR as low as those reported for some mesopelagic environments (e.g., Benavides et al. 2016). Our sensitivity analysis shows that the variability in the $\delta^{15}\text{N}$ and concentration of ambient particulate N were the dominant sources of error in NFR (Table 2).

An alternative detection limit, calculated as the NFR required to produce a change in ^{15}N of 0.00146 atom % (Montoya et al. 1996), produces values similar to our minimum quantifiable rates (Table 2). One reason for our relatively high detection limits is that we used observed particulate N concentrations in the calculations, as originally suggested by Montoya et al. (1996), rather than using the minimum N content required by the mass spectrometer (as in Fernandez et al. 2013). Using relatively low initial $^{15}\text{N}_2$ enrichments ($\sim 3\text{--}4$ atom %, Table 2) further inflates detection limits; however, these low enrichments are a consequence of necessary improvements to the $^{15}\text{N}_2$ assay (Mohr et al. 2010; Wilson et al. 2012). These sensitivity issues highlight the current need for standard reporting of accurate detection limits and a consensus on best practices in N_2 fixation research.

In contrast to the PNW and mesopelagic NPSG, we detected NFR in all surface NPSG and ESP samples (excluding one 75 m NPSG sample; Fig. 2). NFR in the NPSG were within previously reported ranges (Böttjer et al. 2016). In the ESP, the relatively low NFR we report for the gyre ($< 1 \text{ nmol N L}^{-1} \text{ d}^{-1}$) also agree with previous studies (Raimbault and Garcia 2008; Halm et al. 2011). NFR increased near the coast (Fig. 2), and stations 2–5 had rates > 5 times those measured by Dekaezemacker et al. (2013) at nearby stations several months later (April–May 2011). These differences could have arisen from underestimations by Dekaezemacker et al. (2013) due to delayed $^{15}\text{N}_2$ bubble dissolution (Mohr et al. 2010), and/or natural spatiotemporal variability. Previous NFR estimates in upwelling-influenced Chilean and Peruvian waters ranged from undetectable to extremely high ($> 100 \text{ nmol N L}^{-1} \text{ d}^{-1}$) (Raimbault and Garcia 2008; Fernandez et al. 2011, 2015; Loescher et al. 2014) but due to the recent challenges in methodology (Mohr et al. 2010; Dabundo et al. 2014), such comparisons to earlier studies should be treated with caution. Overall, the low to moderate rates we measured add to the mounting evidence that ESP waters are unlikely to harbor the high NFR predicted by initial model projections (Deutsch et al. 2007), perhaps because iron limitation precludes extensive diazotrophy in this region (Weber and Deutsch 2014; Knapp et al. 2016).

Our findings in the ESP point to an emerging paradox: why would N_2 fixation be significant in surface waters where fixed N is available? Ammonium uptake (and to a lesser extent nitrate uptake) is less energetically expensive than N_2 fixation, and conventional wisdom suggests that diazotrophs should only have a competitive advantage over other phytoplankton when N is limiting (Knapp 2012). Yet numerous recent studies have reported NFR in high nitrate waters, often at depth (reviewed in Bombar et al. 2016). In our study, the highest NFR detected in the ESP were at Stn. 1, where nitrate concentrations were also highest (Table 1; Fig. 2), agreeing with other reports of enhanced NFR in upwelled waters (Sohm et al. 2011; Subramaniam et al. 2013). These results suggest that unlike cyanobacteria, heterotrophic

marine NFR might not be reduced in the presence of fixed N (Knapp 2012). Recent culture-based studies support this potential: Bentzon-Tilia et al. (2015) have shown that an alpha-proteobacterial isolate up-regulates N_2 fixation in response to $^{15}\text{NH}_4^+$ additions, possibly as a mechanism for internal redox regulation. Other studies report relationships between heterotrophic N_2 fixation and the supply of dissolved organic matter and hypothesize that organic matter-rich substrates (aggregates) or water masses are necessary to support heterotrophic diazotrophy (Benavides et al. 2015; Severin et al. 2015). Indeed, glucose amendments stimulated detectable NFR in our mesopelagic NPSG samples (Fig. 2). These collective findings help to explain heterotrophic diazotrophy in N-rich waters; however, they are largely correlative and cannot yet constrain the overall importance of heterotrophic diazotrophy to regional or oceanic N budgets.

Challenges in reconciling diazotrophic diversity, abundances, and nitrogen fixation rates

Our cross-ecosystem approach allows us to examine the relationship between diazotrophic genes and NFR in environments with and without measurable N_2 fixation, revealing an apparent negative relationship between diazotrophic diversity and function. The highest *nifH* diversity was observed in PNW samples where N_2 fixation was not detected (Fig. 6), and *nifH* diversity and NFR were inversely related in NPSG and ESP samples (Supporting Information Table S7). This finding is consistent with negative productivity/diversity relationships in many plant and animal communities (Rosenzweig and Abramsky 1993). Competition with successful taxa may lead to a decrease in overall diazotrophic species richness or evenness in environments favoring N_2 fixation.

While it is relatively unsurprising that overall *nifH* diversity does not positively correlate with NFR, we might expect a correspondence between total diazotrophic abundance and NFR based on the cell-specific rates of dominant organisms. We investigated this relationship in the ESP, where a mismatch between cell abundances and NFR has been previously described (Turk-Kubo et al. 2014). Though OTU 2 was the most abundant phylotype in the ESP dataset (Supporting Information Fig. S3), quantification of OTU 2 in our samples revealed low *nifH* concentrations ($1.5 \times 10^2\text{--}4.4 \times 10^3$ *nifH* copies L^{-1} assuming 100% extraction efficiency, Supporting Information Table S5). Using the approach of Turk-Kubo et al. (2014), and assuming the highest-reported cell-specific NFR by heterotrophic marine diazotrophs in culture, a concentration of 9.7×10^4 cells L^{-1} would be required to produce just the ESP-average minimum quantifiable rate (Table 2). Thus, OTU 2 appears insufficient to account for the measured NFR, a finding consistent with previous reports (Turk-Kubo et al. 2014). It is unlikely that this abundance/rate mismatch is driven by an overestimation of NFR due to ^{15}N contamination, since Cambridge $^{15}\text{N}_2$ gas has been observed to

have minimal levels of $^{15}\text{NH}_4^+$ contamination equivalent to rates of $<0.02 \text{ nmol N L}^{-1} \text{ d}^{-1}$ (Dabundo et al. 2014) that are well below our detection limits (Table 2, Supporting Information Table S3). Instead, we believe the abundance of active diazotrophs was underestimated. OTU 2 could have deceptively high relative abundances in the *nifH* sequence dataset due to biases in the degenerate *nifH* primers (Turk et al. 2011) or active diazotrophs in the $>10 \mu\text{m}$ size fraction; if so, this phylotype might not represent the most abundant diazotroph in our samples. Other dominant phylotype(s) or a diverse community of diazotrophs may have contributed to measured NFR. Alternatively, OTU 2 could have extremely high cell-specific NFR, perhaps due to a novel symbiosis. Quantitative PCR reactions performed on a limited number of ESP RNA samples indicate low but detectable *nifH* expression by a gamma-proteobacterial phylotype (ETSP-2, Turk-Kubo et al. 2014) but cannot resolve which diazotrophic taxa drive observed ESP NFR (data not shown).

While the specific organisms driving NFR in the ESP remain elusive, our finding of UCYN-A dominance in the NPSG was consistent among samples (Fig. 4, Supporting Information Fig. S3) and agrees with previous studies (Böttjer et al. 2014). Thus, since the mass ratio hypothesis predicts that the dominant species contributes most to community productivity (Grime 1998), we might expect a positive relationship between UCYN-A abundance and community NFR. However, ddPCR-derived UCYN-A *nifH* gene concentrations did not correlate to NFR in the NPSG ($R^2 = 0.12$, $p > 0.05$). In fact, we are not aware of any studies that have shown strong linkages between molecular estimates of diazotroph cell abundance and NFR in nature. The relationship between gene copies and rates is complicated by species-specific gene copy numbers (Sargent et al. 2016) and gene expression levels (Church et al. 2005b), and also by environmental controls such as light, temperature, nutrients, and dissolved organic matter (Luo et al. 2014; Benavides et al. 2015). Thus, the biogeochemical implications of gene-based diazotrophic abundances should be inferred with caution.

Reconciling the diversity and function of diazotrophic communities is further complicated by the different sensitivities for *nifH* diversity and NFR assays. Our $^{15}\text{N}_2$ tracer incubations produced average minimum quantifiable rates exceeding NFR previously reported in mesopelagic waters (often $<1 \text{ nmol N L}^{-1} \text{ d}^{-1}$, e.g., Dekaezemacker et al. 2013; Rahav et al. 2013; Benavides et al. 2016). Detection limit concerns are further exacerbated by recent reports of $^{15}\text{NH}_4^+$ contaminants in $^{15}\text{N}_2$ gas, which can result in apparent NFR of up to $0.02 \text{ nmol N L}^{-1} \text{ d}^{-1}$ in low-contaminant Cambridge gas stocks and $>100 \text{ nmol N L}^{-1} \text{ d}^{-1}$ in highly contaminated Campro gas stocks (Dabundo et al. 2014). It is not routine for authors to report detection limits for $^{15}\text{N}_2$ fixation rate measurements, yet if the limits we have calculated can be applied widely, then the biogeochemical significance

of diazotrophy may have been overestimated by many studies, particularly in the ESP and the mesopelagic.

While low NFR can be difficult to detect, *nifH* PCR-based methods enable the detection of extremely rare diazotrophs, albeit with potential associated biases and contamination concerns. Since *nifH* sequence data are not quantitative, qPCR is often used to quantify specific diazotrophic phylotypes. This technique has the potential to underestimate total diazotrophic abundance, through mismatches in primer/probe binding sites (Lefever et al. 2013) and because samples are often only screened for specific diazotrophic phylotypes; for example, 4 out of 5 of our most abundant ESP phylotypes would not be targeted using published qPCR primer sets (Supporting Information Table S6). Yet interpretations of qPCR data can also overestimate the functional importance of heterotrophic phylotypes. These organisms are usually detected at concentrations of 10^2 – 10^3 (rarely 10^4) *nifH* copies L^{-1} (Turk-Kubo et al. 2014; Langlois et al. 2015), lower than the cell concentrations required to produce even our minimum quantifiable rates when assuming the highest reported cell-specific NFR from heterotrophic isolates recently cultured by Bentzon-Tilia et al. (2015) (Table 2). In short, it is easier to detect the presence/absence of *nifH* genes than to accurately measure relatively low NFR ($<1 \text{ nmol N L}^{-1} \text{ d}^{-1}$), and the relationship between genes and rates remains elusive.

Conclusions and implications

Here, we illustrate a near-ubiquity of marine diazotrophs—we recovered *nifH* genes from every environment probed—but restricted regions of their functional significance to N cycling. The absence of detectable NFR despite the presence of *nifH* genes in the “unusual” environments of the coastal PNW and mesopelagic NPSG could be due to low diazotrophic abundances or low *nifH* expression by heterotrophic diazotrophs. Our data and others (e.g., Farnelid et al. 2011; Langlois et al. 2015) have begun to map out the biogeography of diazotrophic taxa, indicating a geographical constraint of cyanobacterial diazotrophs and the widespread distribution of putative heterotrophic diazotrophs. Future culture-based efforts can help to determine the ecological controls of these seemingly cosmopolitan heterotrophic diazotrophs and the mechanisms for variability in active N_2 fixation (Bentzon-Tilia et al. 2015). However, the absence of measurable NFR is also related to the inherent sensitivity of the $^{15}\text{N}_2$ fixation assay, a point that is rarely considered in marine N_2 fixation literature despite extensive detection limit calculations in the original paper describing the $^{15}\text{N}_2$ tracer method (Montoya et al. 1996). Our analyses show that this sensitivity issue precludes the detection of very low NFR. Thus, it seems improbable that mesopelagic NFR can accurately be extrapolated to significantly affect the global marine N budget.

References

- Benavides, M., P. H. Moisander, H. Berthelot, T. Dittmar, O. Grosso, and S. Bonnet. 2015. Mesopelagic N₂ fixation related to organic matter composition in the Solomon and Bismarck Seas (Southwest Pacific). *PloS One* **10**: e0143775. Doi:[10.1371/journal.pone.0143775](https://doi.org/10.1371/journal.pone.0143775)
- Benavides, M., and others. 2016. Basin-wide N₂ fixation in the deep waters of the Mediterranean Sea. *Global Biogeochem. Cycles* **30**: 952–961. doi:[10.1002/2015GB005326](https://doi.org/10.1002/2015GB005326)
- Bentzon-Tilia, M., I. Severin, L. H. Hansen, and L. Riemann. 2015. Genomics and ecophysiology of heterotrophic nitrogen-fixing bacteria isolated from estuarine surface water. *Mbio* **6**: e00929–e00915. doi:[10.1128/mBio.00929-15](https://doi.org/10.1128/mBio.00929-15)
- Bombar, D., R. W. Pearl, and L. Riemann. 2016. Marine non-cyanobacterial diazotrophs: Moving beyond molecular detection. *Trends Microbiol.* **24**: 916–927. doi:[10.1016/j.tim.2016.07.002](https://doi.org/10.1016/j.tim.2016.07.002)
- Bonnet, S., J. Dekaezemacker, K. A. Turk-Kubo, T. Moutin, R. M. Hamersley, O. Grosso, J. P. Zehr, and D. G. Capone. 2013. Aphotic N₂ fixation in the eastern tropical South Pacific Ocean. *PloS One* **8**: e81265. doi:[10.1371/journal.pone.0081265](https://doi.org/10.1371/journal.pone.0081265)
- Böttjer, D., D. M. Karl, R. M. Letelier, D. A. Viviani, and M. J. Church. 2014. Experimental assessment of diazotroph responses to elevated seawater pCO₂ in the North Pacific Subtropical Gyre. *Global Biogeochem. Cycles* **28**: 601–616. doi:[10.1002/2013GB004690](https://doi.org/10.1002/2013GB004690)
- Böttjer, D., J. E. Dore, D. M. Karl, R. M. Letelier, C. Mahaffey, S. T. Wilson, J. Zehr, and M. J. Church. 2016. Temporal variability of nitrogen fixation and particulate nitrogen export at Station ALOHA. *Limnol. Oceanogr.* **62**: 200–216. doi:[10.1002/lno.10386](https://doi.org/10.1002/lno.10386)
- Caporaso, J. G., and others. 2010. QIIME allows analysis of high-throughput community sequencing data. *Nat. Methods* **7**: 335–336. doi:[10.1038/nmeth.f.303](https://doi.org/10.1038/nmeth.f.303)
- Church, M. J., D. Jenkins, D. M. Karl, and J. P. Zehr. 2005a. Vertical distributions of nitrogen-fixing phylotypes at Stn ALOHA in the oligotrophic North Pacific Ocean. *Aquat. Microb. Ecol.* **38**: 3–14. doi:[10.1002/lno.10386](https://doi.org/10.1002/lno.10386)
- Church, M. J., M. Short, B. D. Jenkins, D. M. Karl, and J. P. Zehr. 2005b. Temporal patterns of nitrogenase gene (*nifH*) expression in the oligotrophic North Pacific Ocean. *Appl. Environ. Microbiol.* **71**: 5362–5370. doi:[10.1128/AEM.71.9.5362-5370.2005](https://doi.org/10.1128/AEM.71.9.5362-5370.2005)
- Church, M. J., M. Björkman, D. M. Karl, M. A. Saito, and J. P. Zehr. 2008. Regional distributions of nitrogen-fixing bacteria in the Pacific Ocean. *Limnol. Oceanogr.* **53**: 63–77. doi:[10.4319/lo.2008.53.1.0063](https://doi.org/10.4319/lo.2008.53.1.0063)
- Codispoti, L. 2007. An oceanic fixed nitrogen sink exceeding 400 Tg N a⁻¹ vs the concept of homeostasis in the fixed-nitrogen inventory. *Biogeosciences* **4**: 233–253. doi:[10.5194/bg-4-233-2007](https://doi.org/10.5194/bg-4-233-2007)
- Dabundo, R., M. F. Lehmann, L. Treibergs, C. R. Tobias, M. A. Altabet, P. H. Moisander, and J. Granger. 2014. The contamination of commercial ¹⁵N₂ gas stocks with ¹⁵N-labeled nitrate and ammonium and consequences for nitrogen fixation measurements. *PloS One* **9**: e110335. doi:[10.1371/journal.pone.0110335](https://doi.org/10.1371/journal.pone.0110335)
- Dekaezemacker, J., S. Bonnet, O. Grosso, T. Moutin, M. Bressac, and D. Capone. 2013. Evidence of active dinitrogen fixation in surface waters of the eastern tropical South Pacific during El Niño and La Niña events and evaluation of its potential nutrient controls. *Global Biogeochem. Cycles* **27**: 768–779. doi:[10.1002/gbc.20063](https://doi.org/10.1002/gbc.20063)
- Deutsch, C., J. L. Sarmiento, D. M. Sigman, N. Gruber, and J. P. Dunne. 2007. Spatial coupling of nitrogen inputs and losses in the ocean. *Nature* **445**: 163–167. doi:[10.1038/nature05392](https://doi.org/10.1038/nature05392)
- Edgar, R. C. 2010. Search and clustering orders of magnitude faster than BLAST. *Bioinformatics* **26**: 2460–2461. doi:[10.1093/bioinformatics/btq461](https://doi.org/10.1093/bioinformatics/btq461)
- Farnelid, H., and others. 2011. Nitrogenase gene amplicons from global marine surface waters are dominated by genes of non-cyanobacteria. *PloS One* **6**: e19223. doi:[10.1371/journal.pone.0019223](https://doi.org/10.1371/journal.pone.0019223)
- Feely, R. A., S. R. Alin, B. Hales, G. C. Johnson, R. H. Byrne, W.T. Peterson, and D. Greeley. Chemical and hydrographic profile measurements during the 2013 West Coast Ocean Acidification Cruise (WCOA2013, August 3–29, 2013). <http://cdiac.ornl.gov/ftp/oceans/WCOA2013/>. Carbon Dioxide Information Analysis Center, Oak Ridge National Laboratory, US Department of Energy, Oak Ridge, Tennessee. doi:[10.3334/CDIAC/OTG.COAST_WCOA2013](https://doi.org/10.3334/CDIAC/OTG.COAST_WCOA2013)
- Fernandez, C., L. Fariás, and O. Ulloa. 2011. Nitrogen fixation in denitrified marine waters. *PloS One* **6**: e20539. doi:[10.1371/journal.pone.0020539](https://doi.org/10.1371/journal.pone.0020539)
- Fernandez, C. L., and others. 2013. Community N₂ fixation and *Trichodesmium* spp. Abundance along longitudinal gradients in the eastern subtropical North Atlantic. *ICES J. Mar. Sci.* **70**: 223–231. doi:[10.1093/icesjms/fss142](https://doi.org/10.1093/icesjms/fss142)
- Fernandez, C., M. L. González, C. Muñoz, V. Molina, and L. Fariás. 2015. Temporal and spatial variability of biological nitrogen fixation off the upwelling system of central Chile (35–38.5° S). *J. Geophys. Res.* **120**: 3330–3349. doi:[10.1002/2014JC010410](https://doi.org/10.1002/2014JC010410)
- Galloway, J. N., and others. 2004. Nitrogen cycles: Past, present, and future. *Biogeochemistry* **70**: 153–226. doi:[10.1007/s10533-004-0370-0](https://doi.org/10.1007/s10533-004-0370-0)
- Grime, J. 1998. Benefits of plant diversity to ecosystems: Immediate, filter and founder effects. *J. Ecol.* **86**: 902–910. doi:[10.1046/j.1365-2745.1998.00306.x](https://doi.org/10.1046/j.1365-2745.1998.00306.x)
- Großkopf, T., and others. 2012. Doubling of marine dinitrogen-fixation rates based on direct measurements. *Nature* **488**: 361–364. doi:[10.1038/nature11338](https://doi.org/10.1038/nature11338)
- Gruber, N. 2004. The dynamics of the marine nitrogen cycle and its influence on atmospheric CO₂ variations, p. 97–148. In M. Follows and T. Oguz [eds.], *The ocean carbon cycle and climate*. Springer.

- Halm, H., P. Lam, T. G. Ferdelman, G. Lavik, T. Dittmar, J. LaRoche, S. D'Hondt, and M. M. Kuypers. 2011. Heterotrophic organisms dominate nitrogen fixation in the South Pacific Gyre. *ISME J.* **6**: 1238–1249. doi:[10.1038/ismej.2011.182](https://doi.org/10.1038/ismej.2011.182)
- Hewson, I., and others. 2007. Characteristics of diazotrophs in surface to abyssopelagic waters of the Sargasso Sea. *Aquat. Microb. Ecol.* **46**: 15–30. doi:[10.3354/ame046015](https://doi.org/10.3354/ame046015)
- Jayakumar, A., M. Al-Rshaidat, B. B. Ward, and M. R. Mulholland. 2012. Diversity, distribution, and expression of diazotroph *nifH* genes in oxygen-deficient waters of the Arabian Sea. *FEMS Microbiol. Ecol.* **82**: 597–606. doi:[10.1111/j.1574-6941.2012.01430.x](https://doi.org/10.1111/j.1574-6941.2012.01430.x)
- Karl, D., and others. 2002. Dinitrogen fixation in the world's oceans. *Biogeochemistry* **57**: 47–98. doi:[10.1023/A:1015798105851](https://doi.org/10.1023/A:1015798105851)
- Knapp, A. N. 2012. The sensitivity of marine N₂ fixation to dissolved inorganic nitrogen. *Front. Microbiol.* **3**: 374. doi:[10.3389/fmicb.2012.00374](https://doi.org/10.3389/fmicb.2012.00374)
- Knapp, A. N., J. Dekaezemacker, S. Bonnet, J. A. Sohm, and D. G. Capone. 2012. Sensitivity of *Trichodesmium erythraeum* and *Crocospheera watsonii* abundance and N₂ fixation rates to varying NO₃⁻ and PO₄³⁻ concentrations in batch cultures. *Aquat. Microb. Ecol.* **66**: 223–236. doi:[10.3354/ame01577](https://doi.org/10.3354/ame01577)
- Knapp, A. N., L. Casciotti, W. M. Berelson, M. G. Prokopenko, and D. G. Capone. 2016. Low rates of nitrogen fixation in eastern tropical South Pacific surface waters. *Proc. Natl. Acad. Sci. USA* **113**: 4398–4403. doi:[10.1073/pnas.1515641113](https://doi.org/10.1073/pnas.1515641113)
- Kozich, J. J., L. Westcott, N. T. Baxter, S. K. Highlander, and P. D. Schloss. 2013. Development of a dual-index sequencing strategy and curation pipeline for analyzing amplicon sequence data on the MiSeq Illumina sequencing platform. *Appl. Environ. Microbiol.* **79**: 5112–5120. doi:[10.1128/AEM.01043-13](https://doi.org/10.1128/AEM.01043-13)
- Langlois, R., T. Großkopf, M. Mills, S. Takeda, and J. Laroche. 2015. Widespread distribution and expression of Gamma A (UMB), an uncultured, diazotrophic, γ -proteobacterial *nifH* phylotype. *PloS One* **10**: e0128912. doi:[10.1371/journal.pone.0128912](https://doi.org/10.1371/journal.pone.0128912)
- Lefever, S., F. Pattyn, J. Hellemans, and J. Vandesompele. 2013. Single-nucleotide polymorphisms and other mismatches reduce performance of quantitative PCR assays. *Clin. Chem.* **59**: 1470–1480. doi:[10.1373/clinchem.2013.203653](https://doi.org/10.1373/clinchem.2013.203653)
- Letunic, I., and P. Bork. 2016. Interactive tree of life (iTOL) v3: an online tool for the display and annotation of phylogenetic and other trees. *Nucleic Acids Res.* **44**: W242–W245. doi:[10.1093/nar/gkw290](https://doi.org/10.1093/nar/gkw290)
- Loescher, C. R., and others. 2014. Facets of diazotrophy in the oxygen minimum zone waters off Peru. *ISME J.* **8**: 2180–2192. doi:[10.1038/ismej.2014.71](https://doi.org/10.1038/ismej.2014.71)
- Luo, Y.-W., and others. 2012. Database of diazotrophs in global ocean: Abundances, biomass and nitrogen fixation rates. *Earth Syst. Sci. Data* **4**: 47–73. doi:[10.5194/essdd-5-47-2012](https://doi.org/10.5194/essdd-5-47-2012)
- Luo, Y.-W., I. Lima, D. M. Karl, C. A. Deutsch, and S. C. Doney. 2014. Data-based assessment of environmental controls on global marine nitrogen fixation. *Biogeosciences* **11**: 691–708. doi:[10.5194/bg-11-691-2014](https://doi.org/10.5194/bg-11-691-2014)
- Mohr, W., T. Großkopf, D. W. R. Wallace, and J. Laroche. 2010. Methodological underestimation of oceanic nitrogen fixation rates. *PloS One* **5**: e12583. doi:[10.1371/journal.pone.0012583](https://doi.org/10.1371/journal.pone.0012583)
- Moisander, P. H., A. Beinart, M. Voss, and J. P. Zehr. 2008. Diversity and abundance of diazotrophic microorganisms in the South China Sea during intermonsoon. *ISME J.* **2**: 954–967. doi:[10.1038/ismej.2008.51](https://doi.org/10.1038/ismej.2008.51)
- Montoya, J. P., M. Voss, P. Kahler, and D. G. Capone. 1996. A simple, high-precision, high-sensitivity tracer assay for N₂ fixation. *Appl. Environ. Microbiol.* **62**: 986–993.
- Paerl, H. W., M. Crocker, and L. E. Prufert. 1987. Limitation of N₂ fixation in coastal marine waters: Relative importance of molybdenum, iron, phosphorus, and organic matter availability. *Limnol. Oceanogr.* **32**: 525–536. doi:[10.4319/lm.1987.32.3.0525](https://doi.org/10.4319/lm.1987.32.3.0525)
- Rahav, E., E. Bar-Zeev, S. Ohayon, H. Elifantz, N. Belkin, B. Herut, M. R. Mulholland, and I. Berman-Frank. 2013. Dinitrogen fixation in aphotic oxygenated marine environments. *Front. Microbiol.* **4**: 227. doi:[10.3389/fmicb.2013.00227](https://doi.org/10.3389/fmicb.2013.00227)
- Raimbault, P., and N. Garcia. 2008. Evidence for efficient regenerated production and dinitrogen fixation in nitrogen-deficient waters of the South Pacific Ocean: Impact on new and export production estimates. *Biogeosciences* **5**: 323–338. doi:[10.5194/bg-5-323-2008](https://doi.org/10.5194/bg-5-323-2008)
- Riemann, L., H. Farnelid, and G. F. Steward. 2010. Nitrogenase genes in non-cyanobacterial plankton: Prevalence, diversity and regulation in marine waters. *Aquat. Microb. Ecol.* **61**: 235–247. doi:[10.3354/ame01431](https://doi.org/10.3354/ame01431)
- Rii, Y. M., S. Duhamel, R. R. Bidigare, D. M. Karl, D. J. Repeta, and M. J. Church. 2016. Diversity and productivity of photosynthetic picoeukaryotes in biogeochemically distinct regions of the South East Pacific Ocean. *Limnol. Oceanogr.* **61**: 806–824. doi:[10.1002/lno.10255](https://doi.org/10.1002/lno.10255)
- Rosenzweig, M. L., and Z. Abramsky. 1993. How are diversity and productivity related?, p. 52–65. *In* R. E. Ricklefs and D. Schluter [eds.], *Species diversity in ecological communities*. Univ. of Chicago Press.
- Sargent, E. C., A. Hitchcock, S. A. Johansson, R. Langlois, C. M. Moore, J. LaRoche, A. J. Poulton, and T. S. Bibby. 2016. Evidence for polyploidy in the globally important diazotroph *Trichodesmium*. *FEMS Microbiol. Lett.* **362**. doi:[10.1093/femsle/fnw244](https://doi.org/10.1093/femsle/fnw244)
- Schloss, P. D., and others. 2009. Introducing mothur: Open-source, platform-independent, community-supported software for describing and comparing microbial communities. *Appl. Environ. Microbiol.* **75**: 7537–7541. doi:[10.1128/AEM.01541-09](https://doi.org/10.1128/AEM.01541-09)
- Severin, I., M. Bentzon-Tilia, P. H. Moisander, and L. Riemann. 2015. Nitrogenase expression in estuarine

- bacterioplankton influenced by organic carbon and availability of oxygen. *FEMS Microbiol. Lett.* **362**: fnv105. doi:[10.1093/femsle/fnv105](https://doi.org/10.1093/femsle/fnv105)
- Shiozaki, T., M. Ijichi, T. Kodama, S. Takeda, and K. Furuya. 2014. Heterotrophic bacteria are major nitrogen fixers in the euphotic zone of the Indian Ocean. *Global Biogeochem. Cycles* **28**: 1096–1110. doi:[10.1002/2014GB004886](https://doi.org/10.1002/2014GB004886)
- Sohm, J. A., J. A. Hilton, A. E. Noble, J. P. Zehr, M. A. Saito, and E. A. Webb. 2011. Nitrogen fixation in the South Atlantic Gyre and the Benguela upwelling system. *Geophys. Res. Lett.* **38**: L16608. doi:[10.1029/2011GL048315](https://doi.org/10.1029/2011GL048315)
- Subramaniam, A., C. Mahaffey, W. Johns, and N. Mahowald. 2013. Equatorial upwelling enhances nitrogen fixation in the Atlantic Ocean. *Geophys. Res. Lett.* **40**: 1766–1771. doi:[10.1002/grl.50250](https://doi.org/10.1002/grl.50250)
- Turk, K. A., and others. 2011. Nitrogen fixation and nitrogenase (*nifH*) expression in tropical waters of the eastern North Atlantic. *ISME J.* **5**: 1201–1212. doi:[10.1038/ismej.2010.205](https://doi.org/10.1038/ismej.2010.205)
- Turk-Kubo, K. A., M. Achilles, T. R. Serros, M. Ochiai, J. P. Montoya, and J. P. Zehr. 2012. Nitrogenase (*nifH*) gene expression in diazotrophic cyanobacteria in the Tropical North Atlantic in response to nutrient amendments. *Front. Microbiol.* **3**: 386. doi:[10.3389/fmicb.2012.00386](https://doi.org/10.3389/fmicb.2012.00386)
- Turk-Kubo, K. A., M. Karamchandani, D. G. Capone, and J. P. Zehr. 2014. The paradox of marine heterotrophic nitrogen fixation: Abundances of heterotrophic diazotrophs do not account for nitrogen fixation rates in the Eastern Tropical South Pacific. *Environ. Microbiol.* **16**: 3095–3114. doi:[10.1111/1462-2920.12346](https://doi.org/10.1111/1462-2920.12346)
- Weber, T., and C. Deutsch. 2014. Local versus basin-scale limitation of marine nitrogen fixation. *Proc. Natl. Acad. Sci. USA* **111**: 8741–8746. doi:[10.1073/pnas.1317193111](https://doi.org/10.1073/pnas.1317193111)
- Wilson, S. T., D. Böttjer, M. J. Church, and D. M. Karl. 2012. Comparative assessment of nitrogen fixation methodologies, conducted in the oligotrophic North Pacific Ocean. *Appl. Environ. Microbiol.* **78**: 6516–6523. doi:[10.1128/AEM.01146-12](https://doi.org/10.1128/AEM.01146-12)
- Zani, S., M. T. Mellon, J. L. Collier, and J. P. Zehr. 2000. Expression of *nifH* genes in natural microbial assemblages in Lake George, New York, detected by reverse transcriptase PCR. *Appl. Environ. Microbiol.* **66**: 3119–3124. doi:[10.1128/AEM.66.7.3119-3124.2000](https://doi.org/10.1128/AEM.66.7.3119-3124.2000)
- Zehr, J. P., and L. A. McReynolds. 1989. Use of degenerate oligonucleotides for amplification of the *nifH* gene from the marine cyanobacterium *Trichodesmium thiebautii*. *Appl. Environ. Microbiol.* **55**: 2522–2526.
- Zehr, J. P., T. Mellon, and S. Zani. 1998. New nitrogen-fixing microorganisms detected in oligotrophic oceans by amplification of nitrogenase (*nifH*) genes. *Appl. Environ. Microbiol.* **64**: 3444–3450.
- Zehr, J. P., L. Crumbliss, M. J. Church, E. O. Omoregie, and B. D. Jenkins. 2003a. Nitrogenase genes in PCR and RT-PCR reagents: Implications for studies of diversity of functional genes. *Biotechniques* **35**: 996–1013.
- Zehr, J. P., D. Jenkins, S. M. Short, and G. F. Steward. 2003b. Nitrogenase gene diversity and microbial community structure: A cross-system comparison. *Environ. Microbiol.* **5**: 539–554. doi:[10.1046/j.1462-2920.2003.00451.x](https://doi.org/10.1046/j.1462-2920.2003.00451.x)
- Zhang, Y., Z. Zhao, J. Sun, and N. Jiao. 2011. Diversity and distribution of diazotrophic communities in the South China Sea deep basin with mesoscale cyclonic eddy perturbations. *FEMS Microbiol. Ecol.* **78**: 417–427. doi:[10.1111/j.1574-6941.2011.01174.x](https://doi.org/10.1111/j.1574-6941.2011.01174.x)

Acknowledgments

We thank S. Ferrón for MIMS analyses and K. Turk-Kubo for helpful discussions. Support for this project was provided primarily via the Center for Microbial Oceanography Research and Education (EF0424599 D.M. Karl, sub-awards to RML, AW, and JPZ), with additional contributions from the Simons Collaboration on Ocean Processes and Ecology (329108 to D.M. Karl with subaward to AW and JPZ).

Conflict of Interest

None declared.

Submitted 28 September 2016

Revised 19 December 2016

Accepted 14 February 2017

Associate editor: Anya Waite